ACS NANO

www.acsnano.org

ARTICLE

Coordinating an Ensemble of Chemical Micromotors *via* Spontaneous Synchronization

Chao Zhou, Nobuhiko Jessis Suematsu, Yixin Peng, Qizhang Wang, Xi Chen, Yongxiang Gao, and Wei Wang*

Cite This: *ACS Nano* 2020, 14, 5360–5370

Read Online

ACCESS | Metrics & More | Article Recommendations | Supporting Information

ABSTRACT: **Spatiotemporal coordination of a nanorobot ensemble is critical for their operation in complex environments, such as tissue removal or drug delivery. Current strategies of achieving this task, however, rely heavily on sophisticated, external manipulation. We here present an alternative, biomimetic strategy by which oscillating Ag Janus micromotors spontaneously synchronize their dynamics as chemically coupled oscillators. By quantitatively tracking the kinetics at both an individual and cluster level, we find that synchronization emerges as the oscillating entities are increasingly coupled as they approach each other. In addition, the synchronized beating of a cluster of these oscillating colloids was found to be dominated by substrate electroosmosis, revealed with the help of an acoustic trapping technique. This quantitative, systematic study of synchronizing micromotors could facilitate the design of biomimetic nanorobots that spontaneously communicate and organize at micro- and nanoscales. It also serves as a model system for nonlinear active matter.**

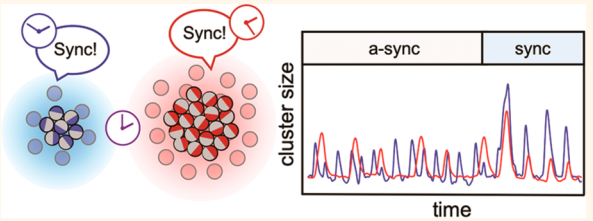

KEYWORDS: *spontaneous synchronization, collective behaviors, micromotors, oscillation, nonlinearity*

The field of nanorobotics is advancing rapidly, especially with untethered, mobile nanorobots that convert environmental energy into self-propulsion.[1−5] Also known as colloidal motors, micromotors, or synthetic microswimmers, they are envisioned to be useful in a wide range of applications, such as biomedicine, environmental monitoring and remediation, and microfabrication.[6−9] Importantly, much of their usefulness hinges on the spatiotemporal coordination of individual microrobots within an ensemble in complex environments.[10,11] For example, upon approaching the target site of a blood clot or tumor, microbots within a swarm might have different speeds, orientation, or phases of activity. Yet, tasks such as drug delivery and removing tissues requires a coordinated effort among microbots, so that tissues can be drilled by a collective force, or drugs can be released simultaneously to reach a threshold concentration. The recent concepts of machines of machines (or robots made of robots) echoes the need for ensemble coordination.[12,13] Such coordination, however, is often achieved through strong external intervention, *e.g.*, complex magnetic fields, that gives microbots exact commands where and when to move.

Nature, however, does it more efficiently and elegantly, often through unsupervised, spontaneous coordination.[14] Typical examples include fireflies flashing in synchrony[15,16] and cardiac cells beating in unison.[17,18] Inspired by these examples, we seek to develop a biomimetic strategy for a group of microbots to communicate, organize, and synchronize *spontaneously*. As will be eluded to later, our proposed strategy is based on the well-known principle of coupled oscillators and is preceded by pioneering studies of synchronized oscillators, ranging from mechanically coupled metronomes[19] and crystal cavities[20] and electrochemically coupled mercury hearts[21−23] to chemically coupled BZ solutions and gels,[24] cardiac cells,[17] and neurons.[25] The particular micromotors we are interested in originated from the Sen group, who demonstrated that microparticles of silver (Ag), silver chloride (AgCl), or silver phosphate (Ag_3PO_4), in the presence of certain chemicals and under illumination, form beating clusters that synchronize with each other.[26−30] These Ag-based oscillators could potentially serve as a prototype of coordinated microbots, yet their functionalities are unfortunately limited by a lack of understanding of

Received: October 24, 2019
Accepted: April 9, 2020
Published: April 9, 2020

https://dx.doi.org/10.1021/acsnano.9b08421
ACS Nano 2020, 14, 5360–5370

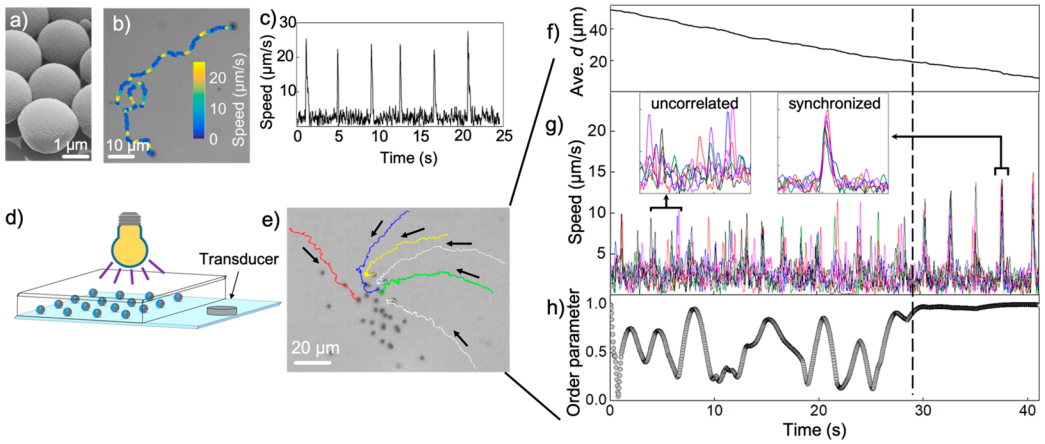

Figure 1. Dynamics of individually oscillating PMMA-Ag micromotors and their synchronization. (a) SEM micrograph of Janus PMMA-Ag particles. (b and c) Pulsating motion of Janus particles in H_2O_2 and KCl and under light. Instantaneous speeds are color-coded in (b) and plotted in (c) for one motor. (d) Schematic of the acoustic setup used for clustering particles. Note that this setup is different from the levitation setup used below in Figure 3. (e) Optical micrograph of an aggregating cluster. Trajectories of six Janus particles aggregating toward the center are plotted for reference. Their average separations, instantaneous speeds, and an order parameter characterizing their synchronization over a period of ~40 s are plotted in (f), (g), and (h), respectively. The dashed line across three panels corresponds to the moment of synchronization. See Methods/Experimental Section for experiment and calculation details.

their unique dynamics and interactions, an issue that we aim to address.

In this article, we report a systematic and quantitative study of the synchronization of oscillating Ag micromotors at both a single-particle and ensemble level, and in doing so we present a robust and tunable model system of synchronizing micromotors, upon which strategies of ensemble coordination can be further developed and interesting nonlinear sciences can be explored. This study uses poly(methyl methacrylate) (PMMA) microspheres half coated with Ag,[31] which move periodically under light and boast clear visualization, better uniformity, and directional propulsion that previous studies lacked. Individually oscillating micromotors are found to synchronize while aggregating into a beating cluster, whose size and beating frequency depend heavily on the competition between phoretic repulsion and acoustic attraction and thus are tunable. Two of such beating clusters also synchronized. Quantification of the synchronization dynamics reveals a transition that is sharply dependent on interparticle (or intercluster) distance. At the end of this article, we discuss some of the fundamental questions that remain to be solved, the relevance of this work to nonlinear sciences, and how the oscillating clusters reported here differ from other dynamic clusters found in the literature.

RESULTS/DISCUSSION

Oscillating Particles and Their Synchronization. Before describing the synchronization among oscillating micromotors, we first review their uncorrelated propulsion and oscillation, which has been described and discussed in detail in our previous study.[31] Understanding this dynamic at a phenomenological level, especially how particles interact with each other, is essential for this article.

The model micromotors being studied here were fabricated by half-coating PMMA microspheres (2.5 μm in diameter, commercially available) with a thin (~50 nm) layer of sputtered Ag (Figure 1a). They are hereafter referred to as PMMA-Ag Janus particles. Previously,[31] we have reported that these PMMA-Ag particles would, in an aqueous solution of H_2O_2 (typically 1−5 wt %) and KCl (typically a few hundred μM) and illuminated by UV or visible light, self-propel away from the Ag hemisphere in a periodic fashion (Figure 1b), making them oscillating micromotors. Quantitatively, this translates to a series of spikes in swimmer speeds, interrupted regularly by long, refractory periods (Figure 1c). Note that other dielectric microspheres, such as polystyrene or SiO_2, could also be used, but Ag is so far an irreplaceable choice of material for oscillation to occur.

In principle, this is not unlike the stick−slip motion of Ag or AgCl microparticles reported by the Sen lab (where our inspirations are drawn),[28] who contributed such an unusual, periodic dynamic to a pair of chemical reactions that alternate on the particle surface:

$$2Ag + H_2O_2 + 2H^+ + 2Cl^- \rightarrow 2AgCl + 2H_2O \quad (1)$$

$$2AgCl + H_2O \xrightarrow{Ag,UV\ light} 2Ag + 1/2O_2 + 2H^+ + 2Cl^- \quad (2)$$

In short, the particle surface oscillates between Ag and AgCl without (quickly) reaching a thermodynamic equilibrium. The net reaction is the decomposition of H_2O_2 into water and O_2.

Building upon this coarse-grained model, we further postulate in a recent study[31] that the production of Ag nanoparticles in eq 2 facilitates further decomposition of AgCl, thus making eq 2 autocatalytic and therefore generating a burst of activity. Ag nanoparticles then slowly convert to AgCl following eq 1 in the presence of H_2O_2, responsible for the resting stages between pulses. Importantly, the production and consumption of ions (and perhaps other neutral species as well) during the oscillation between eqs 1 and 2 produce self-generated gradients and give rise to self-diffusiophoresis,[31,32] which explains the self-propulsion of PMMA-Ag. These oscillating motors also periodically attract and repel charged tracer particles nearby, a testimony of the variation in the magnitude and directions of the chemical gradients. Details of the above descriptions can be found in ref 31.

Having familiarized ourselves with the operating mechanism of one oscillating PMMA-Ag micromotor, we now examine their pairwise interactions and collective behaviors, which, as we will see later, exhibits features of interparticle communi-

https://dx.doi.org/10.1021/acsnano.9b08421
ACS Nano 2020, 14, 5360−5370

cation and synchronization that are critical for coordinating a microbot ensemble.

We begin with oscillating PMMA-Ag micromotors in a dilute suspension (particles at least a few body lengths apart from each other). They pulsate independently with distinct frequencies and phases and with a minimum particle−particle interaction (see Video S1). To induce communication, these oscillating motors were brought closer *via* a simple acoustic trapping device (see Figure 1d for a schematic, and Methods/Experimental Section for details) that collected scattered colloidal particles into a cluster (Video S2). We note that this device did NOT levitate particles (in contrast to our previous acoustic studies[33−35] and to the experiments done in Figure 3),

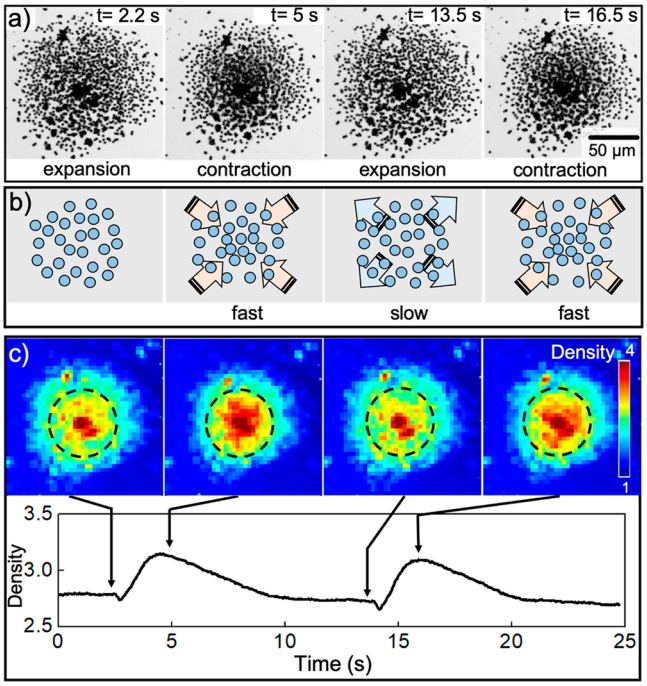

Figure 2. Beating cluster near a substrate. (a and b) Time-elapsed optical micrographs (a) and cartoon schematic (b) of a cluster of PMMA-Ag Janus particles that periodically expands and contracts, taken from Video S3. (c) Particle population density near the cluster nucleus (circled region) periodically changing from being low (more blue) to high (more red). The lowest particle density within the image is set to be 1, corresponding to a dark blue color, to which the other pixels are normalized (a maximum of 4). See Methods/Experimental Section for definition of local density and calculation details.

and particles stayed close to the container substrate. Their gradual aggregation over time is quantified in Figure 1f by a monotonic decrease of their interparticle distance, $d(t)$, calculated by taking average of the distance between one of the aggregating particles (with a coordinate x_i and y_i) and the center of mass of all particles (coordinate x_c and y_c), *i.e.*,

$$d(t) = \frac{1}{N}\sum_{i=1}^{N}[(x_{i,t} - x_{c,t})^2 + (y_{i,t} - y_{c,t})^2]^{1/2} \quad (3)$$

where N is the number of particles.

By tracking the trajectories (Figure 1e) and instantaneous speeds (Figure 1g) of six among ∼25 aggregating PMMA-Ag motors, we find that, while approaching each other, their individual oscillations remained mostly uncorrelated until they were ∼20 μm apart (Figure 1f), beyond which point their oscillation frequencies and phases quickly synchronized within one oscillating period. To quantify this synchronization and to gain an understanding of how it happened, an order parameter was calculated based on the phase differences in the instantaneous speeds among these six oscillating micromotors (Figure 1h, see Methods/Experimental Section for calculation details), where completely synchronized peaks would give an order parameter of 1. As is shown in Figure 1h, the order parameter fluctuated for ∼30 s, beyond which point it reached and remained at 1, indicating synchronization. This is obvious by examining the individual speed profiles of these six particles in Figure 1g, which all collapsed into one peak beyond ∼30 s.

Beating Clusters. As synchronized PMMA-Ag motors continue to aggregate, eventually they form a cluster of oscillating motors, where every motor produces its own chemical field and responds to that from every other motor by being attracted or repelled, all in synchrony. Collectively, this leads to a cluster-wise, periodic expansion and contraction, resembling a beating heart. The phrase "beating cluster" is therefore used hereafter to describe such a cluster that periodically changes in sizes. For example, in Video S3 and Figure 2a, we show two such cycles for a loose cluster of PMMA-Ag particles, located near a substrate, that *rapidly contracts and slowly expands*. A schematic is given in Figure 2b. As a result, the particle density near the beating cluster's nucleus periodically rose and fell, visualized and quantified in Figure 2c (see Methods/Experimental Section for details). We note that the fast rise and slow decay of the local density plot in Figure 2c is qualitatively similar to the areas of a beating cluster shown later in Figure 3d and to the speed profiles of a single oscillating micromotor found in ref 31. This similarity is further discussed later and illustrated in Figure 4b.

Although the oscillation of a cluster seems in qualitative agreement with that of an individual particle, in the sense that both can be divided into a fast stage and a slow stage, one notices an important inconsistency in the ways that particles interact with each other. Specifically, the fast, active stage of a PMMA-Ag micromotor (*i.e.*, speed spikes) is hypothesized to be dominated by the photodecomposition of AgCl (eq 2). According to the theory of ionic diffusiophoresis,[26,27,32,36] eq 2 produces an electric field (because protons diffuse faster than Cl^-) that points toward the particle, which means that negatively charged PMMA-Ag particles would repel each other during the active stages. Collectively, this repulsion among each other would cause a cluster to rapidly *expand*. Yet, we see in Figure 2 that a beating cluster *contracts* more rapidly, opposite to our prediction by diffusiophoresis.

This inconsistency between prediction and experiments is not trivial. The above diffusiophoretic scheme, which relates the surface catalytic reaction to a self-generated electric field and subsequently migration of charged colloids, should hold true for both single particles and their collective behaviors. It constitutes part of our core understanding of oscillatory dynamics and, as discussed further down, will be critical for understanding how these particles are coupled in an ensemble and how synchronization occurs. If a beating cluster is not expanding and contracting in the way as purely phoretic interactions would predict, then what piece of information are we missing?

To reconcile this inconsistency, Altemose *et al.* proposed a hypothesis that the contraction or expansion of a cluster is dominated by an electroosmotic flow rather than particle

https://dx.doi.org/10.1021/acsnano.9b08421
ACS Nano 2020, 14, 5360−5370

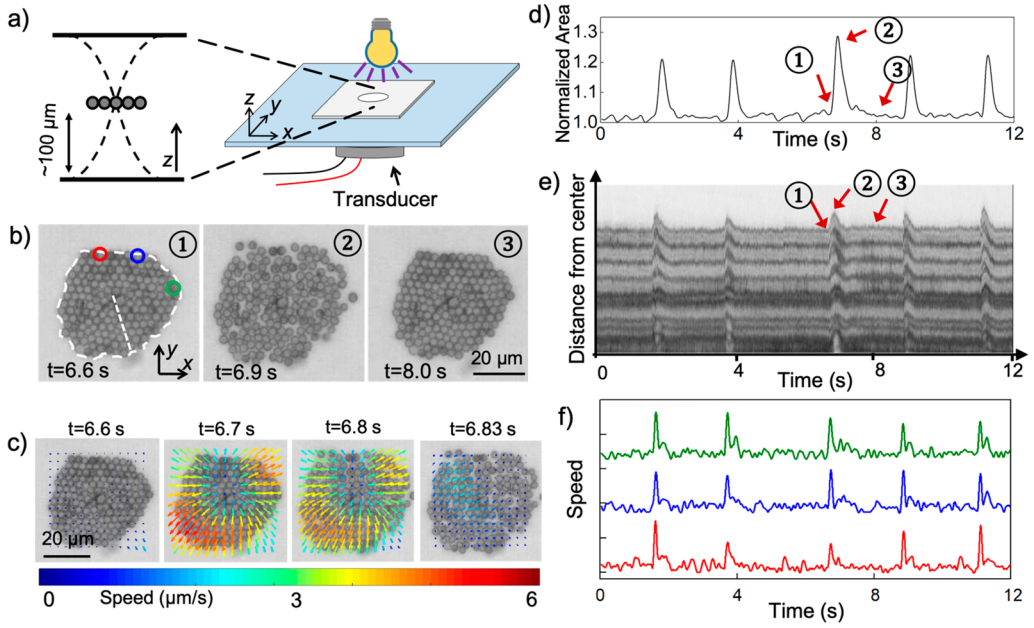

Figure 3. Dynamics of an oscillating, levitated cluster. (a) Schematic of the acoustic setup for levitating PMMA-Ag Janus particles above a substrate. (b) Time-elapsed optical micrographs of a levitated cluster that expands and contracts over time. The numbering corresponds to those in (d) and (e). Three particles along the cluster edge are color-labeled and correspond to the data in (f). The white dashed line corresponds to (e). (c) Mapping of pixel velocities on the expanding cluster in (b), generated by PIV tracking. All pixels are moving radially outward, with the fastest pixels (more red in colors) around the cluster edges. (d) Normalized areas of the beating cluster in (b) show 5 peaks during 12 s. (e) Kymograph of the cutline in (b) over time, revealing 5 cycles of expansion and contraction during 12 s. (f) Instantaneous speeds of three separate Janus particles labeled in (b). Note that (d), (e), and (f) match perfectly in the timing of peaks, barring measurement errors. See Methods/Experimental Section for experiment and calculation details.

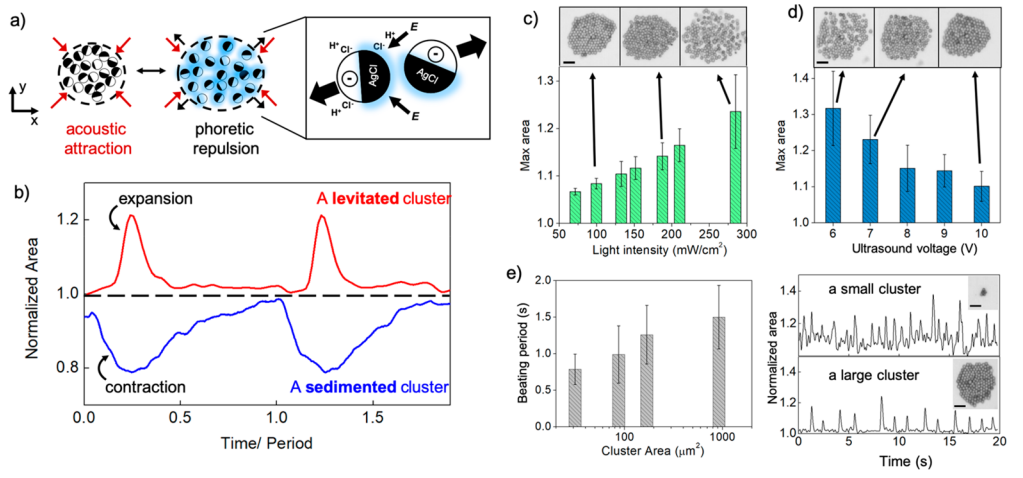

Figure 4. Understanding and tuning the dynamics of a beating cluster. (a) Proposed mechanism for the expansion and contraction of a cluster. It is believed to be subject to two forces (left): a phoretic repulsion (black arrows pointing radially outward) and an acoustic attraction (red arrows that point in). Right: The phoretic repulsion originates microscopically from the phoretic response of Janus motors to the chemical field (illustrated by blue shades) of one another. See the main text for details. (b) The normalized area of a levitated cluster shows that it expands more rapidly than the contraction, whereas the cluster near a substrate (data acquired from Figure 2) undergoes the opposite process. (c and d) The maximum area a cluster can expand to increases with increasing light intensity (c) and with decreasing ultrasound voltages (d). Top panels display optical micrographs of expanded clusters under various conditions. Voltage in (b) was 9 V and light intensity 126 mW/cm^2 in (c). (e) Beating period of a cluster is strongly dependent on its size. Right panels: Oscillating dynamics of two representative clusters of significantly different sizes. All scale bars in Figure 4 correspond to 10 μm.

phoresis.[29] This arises because the cluster we have seen so far, and those reported in the literature, are always located very close (possibly within 1 μm) to a electrically charged glass substrate due to gravity.[34,37,38] The self-generated electric field from an active particle then induces substrate electroosmosis on top of the electrophoresis that we have described above. Because the substrate often carries negative charges, a neighboring particle therefore experiences both an electrophoretic push and a electroosmotic pull, and which way it ultimately moves toward depends on the relative magnitude of the surface zeta potential between the colloids and the wall.[39] This could also happen in our experiments, where electroosmosis near a highly charged glass substrate dominates the interparticle interactions and reverse the cluster dynamics, yet

https://dx.doi.org/10.1021/acsnano.9b08421
ACS Nano 2020, 14, 5360−5370

measuring the surface zeta potential of the substrate is experimentally challenging.[34] An alternative, and better, method to understand the dynamics of a beating cluster requires minimizing the effect of electroosmosis. In addition, a better tunability in the respective contributions of electroosmosis and phoresis is also highly desired.

To meet this request, we have studied the oscillation and synchronization of clusters of PMMA-Ag particles levitated above a substrate. This was achieved by an ultrasonic device that generated acoustic standing waves in megahertz along the z direction (Figure 3a, note that this device is different from that used in Figure 1). As a result, PMMA-Ag particles are levitated onto a nodal plane far from the bottom surface, eliminating the possible contribution by electroosmosis. In addition, secondary acoustic radiation forces (the Bjerknes force)[40−42] are attractive in the x−y plane, serving as an in-plane acoustic trap that collects levitated particles into 2D tight clusters of various sizes. The oscillatory dynamics of one such beating cluster is described in detail in the following. It contained ∼170 particles of PMMA-Ag microspheres, was levitated ∼100 μm above a glass substrate, and subject to 1 wt % H_2O_2, 400 μM KCl, and light illumination of 126 mW/cm^2 (halogen lamp). Under such a condition, this cluster expanded and contracted with a period of ∼1.5 s, and a typical period is shown in Figure 3b and Video S4.

Importantly, a levitated cluster oscillated between a *rapid expansion* and a *slow contraction*, exactly opposite to a cluster oscillating near a substrate shown in Figure 2 (this comparison will again be illustrated in Figure 4b further down). This dynamic is further characterized/visualized in the following three ways, yielding distinct information on its dynamics. First, the velocity map of an expanding cluster in Figure 3c, generated by micro-PIV (see Experimental Section for details), shows a quick, outward motion of PMMA-Ag particles during the first 0.2 s of expansion. Particles near the edge of the cluster moved the fastest, at a peak speed of ∼6 μm/s. The contraction (not shown), in comparison, is much more subdued. Second, the normalized area of the cluster (Figure 3d) rises sharply and periodically (with a period of ∼1.5 s), increasing by ∼20%, then decays slightly and more slowly. The third way is by a kymograph (Figure 3e), which examines the variation over time of the gray scale along a cut line across the radius of the cluster. Because the pixels are significantly different in gray scale between the core of a particle, its edge, and the background, this cut line clearly visualizes the anatomy of a cluster. The generated kymograph in Figure 3e shows five peaks over time, corresponding to the outward and inward motion of the spheres along the cluster radius, in perfect agreement with those acquired from normalized area analysis in Figure 3d.

In addition to understanding dynamics of a whole cluster, the above analysis also reveals interesting behaviors of individual PMMA-Ag particles within such a cluster. First, all PMMA-Ag particles oscillated simultaneously with synchronized frequencies and phases. This is clear from Figure 3f, which tracks the instantaneous speeds of three separate PMMA-Ag particles along the edge of a beating cluster (color-labeled in Figure 3b). Although separated by at least three particle diameters and thus not directly interacting with each other, these three particles oscillated in almost perfect synchrony. This leads to the second point, which is that particles always moved outward along the radial direction of a cluster regardless of their positions within a cluster or their own orientations (suggested by Figure 3c and e). This is in stark contrast to their uncorrelated motion that always pointed away from the Ag hemisphere, such as those in Figure 1b. Finally, when a cluster is expanding, particles near its edge escaped farther than those trapped within. This is visualized by the velocity map in Figure 3c and again by the kymograph of Figure 3e that shows higher peaks farther away from the center (*i.e.*, intensity lines farther up along the y axis in Figure 3e). These results on individual particles within a cluster suggest that a global field (or fields) is responsible for the collective motion of particles. The nature of this field will be discussed in the next section.

Understanding and Tuning Cluster Dynamics. The periodic expansion and contraction of a levitated cluster of PMMA-Ag particles *in the absence of electroosmosis*, shown in Figure 3, can be qualitatively understood by the following phenomelogical model that involves a competition between phoretic repulsion and acoustic attraction (illustrated in Figure 4a). Microscopically, the chemical gradient of one active PMMA-Ag particle, as a result of the photodecomposition of AgCl (eq 2), gives rise to an inward electric field. Its neighbors, being negatively charged, then move away from this electric field. This phoretic repulsion is mutual and causes PMMA-Ag particles to scatter. In a tight cluster, the chemical gradients of every active PMMA-Ag particle overlap to produce an electric field that points in toward the cluster center. All PMMA-Ag particles then respond to this electric field by collectively moving outward rapidly. Reversing this chemical reaction reverses the electric field and leads to contraction. This phoretic mechanism is strongly supported by the reversal of expansion and contraction of a cluster before and after being levitated (see Figure 4b for a comparison), providing yet another testimony of the usefulness of acoustic levitation in identifying the substrate effect in the study of micromotors, as we have recently shown in a few studies.[33,45,51]

The presence of a global mean field responsible for the collective behaviors of a beating cluster is supported by two additional control experiments. First, we confirm that the presence of inert tracer microspheres (2 μm polystyrene or SiO_2 microspheres) or SiO_2 microrods (∼3 μm long and 300 nm in diameter) mixed with active Janus microspheres does not qualitatively alter the dynamics of a now mixed cluster (near a substrate), nor does the mixture phase separate. This observation suggests a mean field gradient that operates on every particle in a cluster, active or not, consistent with the mechanism described above. In addition, we confirm that pure Ag microspheres, instead of PMMA-Ag Janus microspheres, form beating clusters that show qualitatively the same behaviors as those formed by their Janus counterparts (see Figures S1 and S2). This similarity suggests that a Janus particle in a cluster can no longer "feel" its orientation, as the global field dominates over the individual gradient of each particle in a beating cluster.

On top of the phoretic interactions, an additional acoustic attractive force (the Bjerknes force) *constantly* pulls all particles toward the cluster center. It then acts as a resistance when the cluster expands, limiting its maximum size, while as an assistance when the cluster contracts. In fact, we believe the Bjerknes force is stronger than the attraction caused by phoretic interactions and is the leading reason that a levitated, expanded cluster is able to contract to full compactness. This argument, that eq 1 produces a weak, phoretic attraction, is supported by an experiment where, under weak acoustic forces,

https://dx.doi.org/10.1021/acsnano.9b08421
ACS Nano 2020, 14, 5360−5370

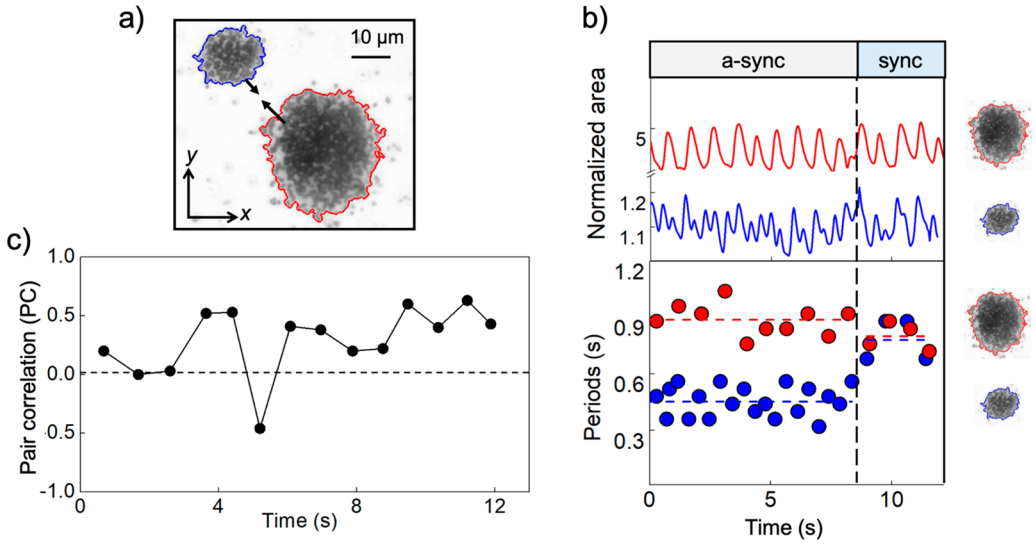

Figure 5. Synchronization between two beating clusters (Video S6). (a) Optical micrographs of one large and one small beating cluster approaching each other, both levitated by ultrasound. The colors of the cluster outlines correspond to the coloring of data plots in (b). (b) Synchronization kinetics. Normalized areas (top) and change in oscillating periods (bottom) of two clusters are plotted over time. The synchronization of these two clusters occurred at t = ~8 s, indicated by the vertical dashed line. (c) Pair-correlation (PC) between the red and blue curves in (b), showing a poor and fluctuating correlation until ~8 s. Note that these clusters are made of Janus particles of 1 μm in diameter, rather than 2.5 μm, because they form clusters that are easier to manipulate by ultrasound.

the levitated cluster was not able to contract to the compact form but instead slowly grew in size over a few cycles of oscillation (results not shown). Furthermore, this argument also applies to a nonlevitated cluster above a substrate (Figure 2), where a cluster was able to contract to compactness in every cycle only because of the presence of electroosmotic flows that reversed the directionalities of these two processes. It is the expansion, corresponding to eq 1, that is weak in this sedimented case.

A levitated, beating cluster can then be regulated by tuning the relative magnitude of the above two forces, phoretic repulsion and acoustic attraction, as demonstrated in Figure 4b and c and Video S5. For example, increasing the light intensity presumably accelerated the photodecomposition of AgCl, leading to a larger chemical flux, stronger phoretic repulsion, and thus a more expanded cluster (Figure 4c). Increasing the ultrasound voltage, on the other hand, increases the attractive Bjerknes force and leads to tighter clusters (Figure 4d) (Note that acoustic forces and phoretic interactions operate by different principles, with hydrodynamics that likely decay differently over distance. This difference, however, does not qualitatively change the discussion here.) An interesting possibility is that, instead of keeping the light intensity or ultrasound voltage constant, as is typically done in our experiments, both parameters can be varied over space and time, possibly generating more complicated cluster dynamics. This will be worth exploring in the future.

An interesting result is that the dynamics of a beating cluster is also dependent on its size. Video S5 and Figure 4e show that four independent clusters found in the same experiment oscillate with significantly different periods, with the smallest one beating about twice as fast as a second cluster roughly 100 times larger. A similar trend has been reported by Altemose *et al.* on oscillating clusters of Ag_3PO_4 particles.[29] Tentatively, we hypothesize that such a size-dependence of the periods of oscillating clusters is related to the reaction-diffusion of certain chemicals involved in the oscillation and the recovery time for the refractory periods. For example, eq 1 (the oxidation of Ag into AgCl) is believed to be the slow step,[29] and the concentration of H_2O_2 therefore regulates the period of the oscillation (as was shown in our study of an individual PMMA-AgCl oscillator).[31] A larger cluster consumes H_2O_2 more and might lead to a low local concentration of H_2O_2 that increases its period.

What happens for even larger oscillating clusters? We do not have the answer, as experiments become technically challenging for very large clusters. However, it is reasonable to speculate that a qualitative change of the cluster dynamics might occur, such as a complete stoppage of oscillating, emergence of additional synchronization centers, or a transition to a directional motion. Such a dramatic change in the behavior caused by a continuous increase in the population is a well-known phenomenon called "quorum sensing", which has been studied extensively in biology and in synthetic oscillators,[14,43−45] where a change in population size, even a slight one, could dramatically alter the population dynamics and cause emergent behaviors such as waves.[46] For example, both camphor boats[47] and yeast cells[44] are known to undergo a transition from continuous to oscillatory state as their number density is increased. This issue pertains closely to applications of swarms that contain many microbots and will be explored in the future.

Synchronization of Two Beating Clusters. Just like an oscillating PMMA-Ag motor, a beating cluster can also synchronize with its neighbors. This was first reported by Altemose *et al.*, who showed that a number of clusters of Ag_3PO_4 microparticles scattered across the field of view oscillated in phase-shifted synchrony.[29] However, the kinetics of synchronization as two asynchronized clusters are brought together remains unknown. As we have shown in the last section, clusters of different sizes beat in different frequencies and are thus a good model system for examining synchronization between two populations of oscillators that are already locked to their own frequencies, *i.e.*, two beating clusters.

https://dx.doi.org/10.1021/acsnano.9b08421
ACS Nano 2020, 14, 5360−5370

We examine the synchronization of two beating clusters levitated by ultrasound (Figure 5, calculated with the first 20 s of Video S6). Initially, one small cluster oscillating with an average period of ∼0.45 s (blue in Figure 5a) was located far away from a second cluster 4 times as large with a period of 0.89 s (red in Figure 5a). Under the attractive Bjernkes force they slowly approached each other, while their oscillating frequencies and phases remained largely independent ("a-sync" stage in Figure 5b). As their intercluster distance decreased below a few micrometers, they quickly synchronized ("sync" stage in Figure 5b).

Pair-correlation (PC) was calculated to quantify the synchronization between the two beating clusters. To calculate the correlation, the time series of the area of each cluster (Figure 5b) was first normalized by their respective maximum area during expansion. Then, the correlation between the normalized areas of two clusters for each period of the larger cluster was calculated using the following equation:

$$\mathrm{PC} = \frac{\langle (A_l - \overline{A_l})(A_s - \overline{A_s})\rangle}{\sqrt{\langle (A_l - \overline{A_l})^2\rangle \langle (A_s - \overline{A_s})^2\rangle}} \quad (4)$$

where $\overline{A_l}$ and $\overline{A_s}$ are the averaged area in each period of the large and small cluster, respectively. The value of PC fluctuated between −0.5 and 0.5 up to ∼9 s, beyond which point PC stabilized around 0.5 ± 0.1, indicating synchronization (it is not strictly 1 because correlation is very sensitive to small differences between data). Note that, not unlike those six oscillating Janus particles in Figure 1 that synchronized while approaching each other, the clusters shown here synchronized their oscillations as they gradually approached each other, resulting in a coupling strength that varied over time. This feature is discussed later.

Key Features Operating at Different Scales. Throughout this study we have described dynamics at three levels: a single oscillating particle, a cluster made of many such particles, and a pair of beating clusters. At all three levels we see oscillating entities interacting with each other and synchronizing, unified by a central theme of chemically coupled oscillators. To further clarify, we briefly review the key features operating at each level, while highlighting a few fundamental questions that still linger.

First, at an individual level, a PMMA-Ag Janus particle is assumed to undergo a chemical oscillation on its surface, and a burst of outward chemical flux propels it forward. Two of such active particles couple to each other by reciprocally attracting and repelling each other through phoretic interactions and more importantly by interrupting and resetting each other's clock. This is most likely achieved *via* coupling with chemical fields (detail unknown), making them chemically coupled micromotors.

As the population of Janus particles becomes larger and denser, their coupling becomes stronger, and the chemical gradient overlaps to generate a mean field. A strongly coupled cluster then expands and contracts in unison, disregarding the intrinsic dynamics or orientations of each constituent particle. Notably, the oscillating periods and magnitude of an uncorrelated particle is different from the cluster they form, possibly reflecting a variation in the concentrations of chemicals.

As oscillating clusters meet each other, they again behave as chemically coupled oscillators, now with a chemical field that is more isotropic and farther-reaching than a single Janus particle. However, synchronization between two clusters did not occur until they were surprisingly close, possibly because a cluster was more firmly entrained to its own frequency and phase and thus resisted changes more strongly than a single particle. An interesting experiment would be to arbitrarily tune the intercluster distance. Yet, this has proven difficult for the acoustic trapping technique we used, because of the technical challenge associated with generating local traps that manipulate individual clusters, rather than the global trap we currently employ. Other trapping techniques, such as optical traps, might be worth exploring.

One of the most important missing pieces in our reasoning is the nature of the "coupling". Specifically, how do the chemicals that one particle consumes and produces change the reactions of a second particle and resets its chemical clock? Moreover, what exactly is being sent and received, as the critical signaling agent? We note that a similar coupling effect was achieved by various ways in earlier studies of natural or synthetic oscillators. For example, BZ oscillators couple by the diffusion of activator and inhibitor species,[45] and oscillating cells such as cardiac pacemaker cells and neurons couple by the diffusion of Na^+ and K^+, which affects their trans-membrane potential.[18,25] Mercury beating hearts synchronize by electrochemical coupling,[21] and so do Ni electrodes in H_2SO_4.[48] Metronomes sense each other by mechanical forces. The synchronization observed on the catalysis of CO oxidation on a Pt(111) surface is partly due to the surface diffusion of mobile adsorbates that induce surface reconstruction.[49] None of these coupling mechanisms, however, can be simply mapped to our observations. Although we have some premature guesses that involve reaction-diffusion of chemicals such as Ag^+, Cl^-, H^+, and H_2O_2, conclusive proofs and a definite mechanism are not yet available. This is clearly a top priority for subsequent studies.

Another prominent phenomenon we frequently observe with oscillating microparticles is the emergence of traveling waves, manifested in the collective migration of particles in sequence. This is not discussed here in detail, because the rich dynamics of waves deserves its own dedicated study. However, we do note that the generation of waves is a hallmark feature of chemical coupled oscillators, commonly observed across a wide range of natural or synthetic oscillators.[50,51] The synchronization of oscillating entities, and the finite rate of a signaling agent transmitting across the population, naturally gives rise to waves. This also suggests that the dynamics of waves, such as their speeds and periods, can reveal important information on the chemical reactions underlying oscillations and synchronization, such as the nature of the diffusing species. This aspect is currently being pursued in our lab and will be published separately.

Relevance to Coupled Oscillators and Nonlinear Sciences. In addition to being a prototype of communicating microbots, the current Ag-based oscillating system can be potentially developed into a good model system for the study of nonlinear sciences. One beauty of this model system is that it is driven most likely by heterogeneous reactions, thus can be engineered on a wide selection of surfaces. Its dynamics are also highly sensitive to, and tunable by, experimental parameters such as chemical concentrations and light intensity, offering a wide phase space of dynamics. This model system is also likely mathematically describable.[52] An example is given in the Supporting Information, where the synchronization

https://dx.doi.org/10.1021/acsnano.9b08421
ACS Nano 2020, 14, 5360−5370

between two beating clusters can be described by a Kuramoto-like model.

Two interesting prospects emerge for future studies in the realm of nonlinear sciences. One opportunity arises where intentionally tuning the coupling strength between these oscillators could affect their capability to synchronize and to demonstrate other collective behaviors. In addition to the obvious method of tuning the chemical activity, the Kuramoto model predicts synchronization, provided sufficiently strong coupling, even in an inhomogeneous population with small differences in their natural frequencies.[52] It is then curious to see to what extent can a unified group defend itself from the presence of "impurities" or "defects", a scenario possibly probed by an experiment with a binary mixture of Janus motors of different oscillating frequencies. In the context of an ensemble of microbots, this question relates to the situation where some members of the group are "different" from others, a common heterogeneity arising from fabrication imperfections, or the way each motor interacts with the highly heterogeneous environment. Whether a heterogeneous group like this can still synchronize is then of practical concern.

A second opportunity is related to the mathematical model called "swarm oscillator", which has been recently proposed to describe coupled oscillators that vary their coupling strength while self-propelling.[53,54] A notable example of swarm oscillators is a social amoeba that excretes and receives chemoattractant, forms spiral waves, and migrates by chemotaxis.[55] In a recent study, O'Keeffe *et al.* predicted a number of interesting states of collective behaviors for swarm oscillators, including static sync and phase waves.[56] These phases are yet to be discovered in experiments. The concept of swarm oscillators matches well with coordinated microbots that often move in swarms. The current study therefore sheds light on bridging these two concepts together.

Comparison to Reports of Dynamic Colloidal Clusters. Finally, we compare the oscillating clusters reported here to earlier studies of clusters that change sizes. Prominent examples include a micro-"firework", where a cluster of TiO_2 or AgCl microparticles explodes upon UV light exposure, but slowly contracts back to a tight cluster after light is turned off.[26,57,58] A similar effect has also been observed with clusters of various types of microparticles levitated by ultrasound and exposed to UV light.[59] Adding or removing NH_3 from a suspension of Ag_3PO_4 microparticles also triggers a reversible transition in their aggregation states.[27] Ensembles of photoactive microparticles have also been shown to self-assemble into close-packed crystalline clusters under light, which then dissolve when lighting is removed.[60,61]

On a superficial level, all these clusters oscillate between an expanded and a contracted state, similar to what is reported here. However, one distinct feature of an oscillating cluster is that it does so in a spontaneous, uninterrupted, and highly regular fashion, without a change in experiment condition or human intervention (best illustrated in Figure 2). This is fundamentally different from previous demonstrations of "dynamic" clusters, where every instance of expansion or contraction must be triggered externally, in the form of adding/removing chemicals or turning on/off light. Even though spontaneously oscillating clusters studied here are not necessarily superior to triggered ones reported previously, we note that naturally occurring dynamic systems are often self-sustained and adaptive, and this study is one step toward bringing that feature to man-made micromachines and smart materials in general.

CONCLUSIONS

To summarize, we have quantitatively examined how the uncorrelated oscillatory motion of PMMA-Ag Janus micromotors, and the clusters that they form, can synchronize. Coupling among these oscillating entities can be partially and qualitatively understood by a mean chemical field arising from the overlapping of nearby active particles. Its gradient then couples to the charged substrate and produces electroosmosis, which gives rise to a cluster of oscillating colloids that expands and contracts. Finally, quantification of the synchronization process at both an individual and ensemble level reveals that the coupling strength is strongly dependent on interparticle or intercluster distance.

Moving forward, a number of topics are worth exploring. For example, the coupling mechanism underlying synchronization remains poorly understood. Future efforts will focus on identifying the chemical species produced from an oscillating particle/cluster and quantifying their distribution, as well as on mapping the electric fields and fluid flows. Second, although we have used PMMA-Ag oscillating micromotors as an example, other micromotors of different, nonlinear dynamics could in principle show similar synchronization provided a means to couple. Examples are, however, rare.[47] Third, the chemical signals responsible for the synchronization takes time to propagate, leading to the possible emergence of waves, which will be the focus of our next endeavors.

Standing on the shoulders of earlier experimental demonstrations of oscillating particles and clusters, the findings reported here represent a significant progress in understanding, as well as the capability in controlling, the coordination of a group of micromachines. We anticipate that the knowledge acquired from this study will inspire future designs of intelligent materials and usher in opportunities for the studies of nonlinear sciences. In addition, although microscopic particles are explored in the current study, there is no fundamental limitation that prevents applying the same operating principles to nanoscopic systems as well.

METHODS/EXPERIMENTAL SECTION

Sample Fabrication. A monolayer of PMMA microspheres (2.5 μm diameter, BangsLab) was formed at the water−hexane interface and transferred to a wafer, following a previously reported protocol.[62] PMMA-Ag Janus spheres were fabricated by evaporating a 50 nm layer of silver on the monolayer using an e-beam evaporator. These particles were redispersed by sonication and stored in water for motor experiments. We note that the quality of the silver layer is critical for the success of oscillation experiments. In our lab, we tend to use freshly prepared samples and store them in vacuum desiccators for a prolonged time. Experiments on oscillation and synchronization can also be reproduced with Janus particles made with polystyrene or SiO_2 microspheres, but we have observed a better consistency for particles made with PMMA microspheres.

Motor Experiments. In a typical experiment, an aqueous suspension of PMMA-Ag particles with predetermined concentrations of H_2O_2 and KCl was transferred into a rectangular capillary glass tube (Vitrocom No. 3520-050, thickness of ~200 μm) by capillary forces. This capillary tube was then observed with an inverted optical microscope (Olympus IX71) or an upright microscope (Olympus BX51) in experiments where particles were levitated. Optionally, transducers are mounted on the microscope for ultrasound experiments (see Ultrasound Experiment section for details). A mercury lamp (Olympus USH-103OL(C)), halogen lamp (Olympus 12

https://dx.doi.org/10.1021/acsnano.9b08421
ACS Nano 2020, 14, 5360−5370

V100W HAL-L(C)), or LED UV lamp (Thorlabs, M365LP1-C1, operating at 365 nm) was used in different experiments, and samples were typically illuminated from above. Light intensities were measured with a power meter (Thorlabs, PM100A+S175C). Videos were recorded with a CMOS camera (FLIR GS3-U341C6C-C, Point Gray) typically at 30 frames per second (fps).

Tracking Motors and Clusters. Single-particle tracking was achieved by MATLAB codes provided by Hepeng Zhang's lab at Shanghai Jiaotong University. In general, each particle was first distinguished from the background *via* a gray value threshold, and their coordinates were extracted and used to calculate the instantaneous particle speeds. We note that a variety of programs, both commercial and open source, are available online that can be used to achieve in principle the same tracking results as what we obtained.

Population density of an oscillating cluster in Figure 2c was calculated as follows. An optical micrograph is first converted to gray scale with imageJ (https://imagej.nih.gov/ij/) and then meshed into square elements of 20 × 20 pixels (0.26 μm/pixel). The mean gray value of each element is then calculated and assigned to all pixels within this element. After this process, we acquire a coarse-grained image with averaged local pixel gray values, which are then normalized to the lowest gray value of the image and color coded. This normalized value is defined as the local population density, ranging from 1 to 4. In addition, a circular area marked in Figure 2c was also selected, and the mean gray value within this area was calculated over time as shown in the bottom panel in Figure 2c. We note that areas where particles are denser appear darker in an optical micrograph and give a smaller gray value because in imageJ a bright pixel gives a higher gray value than a dark pixel (gray value ranges from 0 to 255 for pure black to white). To avoid confusion, we have subtracted 255 by the measured gray value and used the difference to calculate the density of circled areas so that *a higher gray value corresponds to a denser area*.

To calculate the area of a beating cluster such as that shown in Figure 3, the micrograph is first processed by imageJ so that the cluster is distinguished from its background by tuning the gray value threshold carefully. The cluster area was then calculated by MATLAB codes and normalized. Peaks of normalized area profile over time were extracted, and then the max areas and periods were calculated for Figures 4 and 5.

Micro-PIV of a beating cluster in Figure 3c was achieved by MATLAB and Fluere software (http://fluere.kplynch.com/). A video of a beating cluster was first decomposed into images, and the contrast was enhanced. Images were then analyzed by Fluere, and speed data in the x and y direction at each point (13 × 13 point in Figure 3c) were generated. Then, the data were processed by MATLAB, and speed arrows were plotted by overlapping the original video. The length and color of the arrows both indicate the magnitude of the local speeds (longer and more red arrows indicate high local speeds).

Ultrasound Experiment. *1. Particle Trapping and Aggregation on a Substrate.* This procedure corresponds to Figure 1d. A rectangular capillary tube filled with micromotors and 0.5 wt % H_2O_2 and 200 μM KCl was attached on the center of a rectangular glass coverslip *via* ultrasound coupling gel. The capillary tube was placed perpendicular to the long axis of the coverslip, and an ultrasonic transducer (Steminc Inc., SMD12T06R412WL, resonance frequency 3.4 MHz) was attached on the coverslip with ultrasound gel next to the capillary tube. UV light at 365 nm and of 134 mW/cm^2 intensity was applied from above. Note that the sketches in Figure 1d and 3a are solely for the purpose of illustrating the experimental setup, and components are not drawn accurately or to scale.

To induce the aggregation of individually oscillating particles (Figure 1d), sound waves of frequency ∼3.9 MHz were produced by the transducer driven by a waveform generator (Keysight 33210A) at 10 V voltage. At this condition, particles gradually aggregated as a result of the acoustic radiation force. They did not levitate, partly because the transducer was attached to the side, rather than the bottom, of the experimental chamber. In addition, the operating frequency was slightly off the resonance frequency required to achieve levitation.

2. Levitating Clusters. This procedure corresponds to Figure 3a. To levitate particles and clusters far from the substrate, an ultrasonic transducer was attached to the bottom of a silicon wafer by ultrasound gels. A rectangular capillary tube with PMMA-Ag microspheres and 1 wt % H_2O_2 and 400 μM KCl was attached on the shiny side of the wafer, directly above the transducer center. Sound waves of frequency ∼3.8 MHz were produced by the transducer, creating a standing wave and a nodal plane at the middle of the capillary tube. This plane is ∼100 μm above the substrate.

PMMA-Ag microspheres, responding to an acoustic radiation force, were levitated from the bottom of the chamber toward the nodal plane, on which they migrated laterally toward the pressure minimum. While migrating, 2D clusters of various sizes form due to the presence of in-plane secondary radiation forces (also known as Bjerknes forces) that were attractive among particles. The same attractive force is also responsible for the approaching of clusters shown in Figure 5.

The voltage was fixed at 9 V in experiments with varied light intensities (Figure 4c), but was tuned from 6 to 10 V in the experiment of tuning cluster dynamics (Figure 4d). Particles were observed with an upright microscope, and visible light was produced by a halogen lamp with intensity ranging from ∼60 to 280 mW/cm^2, irradiating from above. In the study of synchronization of two beating clusters, a mercury lamp was used operating at 387 mW/cm^2.

Data Analysis for Synchronization of Six Micromotors. In order to quantify the synchronization of the oscillatory motion of individual motors, we calculated a Kuramoto order parameter, shown in Figure, 1h. This is done by first defining phase, θ, for each oscillator. Because the particle behaviors were intermittent, it was hard to define the phase for each instantaneous speed, v. Instead, we focused on the speed peaks and defined them as $\theta = 0$ (or 2π). Phases in between were calculated by linear interpolation. More specifically, to define the phase values, the time instance of the ith peak, t_i, was obtained at first, for which the phase value was defined as 0 or 2π. Then, phase value $\varphi(t)$ at arbitrary time $t_i < t < t_{i+1}$ was defined by linearly interpolating between $\varphi(t_i)$ and $\varphi(t_{i+1})$ with the following equation:

$$\phi(t) = 2\pi \frac{t - t_i}{t_{i+1} - t_i} \tag{5}$$

Using these phase values, the Kuramoto order parameter R was calculated for each time instance by the following equation:[59]

$$\frac{1}{N}\sum_{j=1}^{N} \exp(i\phi_j(t)) = R\,\exp(i\theta) \tag{6}$$

Here, N is the number of oscillators. The order parameter R can be considered as the position of the center of mass of the oscillators in the phase space.

We selected six particles in Figure 1e and calculated the Kuramoto order parameter for each time instance using the above method. Noise is removed by setting a threshold value for the peak speed to 5 μm/s so that only the peaks above the threshold value were analyzed. In addition, if there were more than one peak within 1 s (well within one oscillation period), the maximum speed peak was taken and other peaks were considered noise and ignored.

ASSOCIATED CONTENT

Supporting Information

The Supporting Information is available free of charge at https://pubs.acs.org/doi/10.1021/acsnano.9b08421.

Video S1: Micromotors pulsate independently with distinct frequencies and phases (AVI)

Video S2: Aggregation of six oscillating Janus micromotors and their synchronization (AVI)

Video S3: A beating cluster on a substrate (AVI)

Video S4: A levitated beating cluster (AVI)

https://dx.doi.org/10.1021/acsnano.9b08421
ACS Nano 2020, 14, 5360−5370

Video S5: Levitated clusters of different sizes oscillating under various light intensities and ultrasound driving voltages (AVI)

Video S6: Synchronization of two levitated, beating clusters (AVI)

Experiments with pure Ag microspheres, calculation of synchronization between two beating clusters (PDF)

AUTHOR INFORMATION

Corresponding Author

Wei Wang − *School of Materials Science and Engineering, Harbin Institute of Technology (Shenzhen), Shenzhen 518055, China;* orcid.org/0000-0003-4163-3173; Email: weiwangsz@hit.edu.cn

Authors

Chao Zhou − *School of Materials Science and Engineering, Harbin Institute of Technology (Shenzhen), Shenzhen 518055, China*

Nobuhiko Jessis Suematsu − *School of Interdisciplinary Mathematical Sciences, Graduate School of Advanced Mathematical Sciences, and Meiji Institute for Advanced Study of Mathematical Sciences (MIMS), Meiji University, Nakano-ku, Tokyo 164-8525, Japan;* orcid.org/0000-0001-5860-4147

Yixin Peng − *School of Materials Science and Engineering, Harbin Institute of Technology (Shenzhen), Shenzhen 518055, China*

Qizhang Wang − *School of Materials Science and Engineering, Harbin Institute of Technology (Shenzhen), Shenzhen 518055, China*

Xi Chen − *School of Materials Science and Engineering, Harbin Institute of Technology (Shenzhen), Shenzhen 518055, China*

Yongxiang Gao − *Institute for Advanced Study, Shenzhen University, Shenzhen 518060, China;* orcid.org/0000-0003-4042-0248

Complete contact information is available at: https://pubs.acs.org/10.1021/acsnano.9b08421

Notes

The authors declare no competing financial interest.

ACKNOWLEDGMENTS

We are grateful for the helpful discussions with Ayusman Sen, Thomas Mallouk, Darrell Velegol, Igor Aranson, Jie Zhang, Zexin Zhang, Mingcheng Yang, and Hepeng Zhang. We also acknowledge the help with MATLAB codes for particle tracking from Hepeng Zhang's lab. This project is financially supported by Natural Science Foundation of Guangdong Province (No. 2017B030306005), the National Natural Science Foundation of China (11774075 and 11402069), the Science Technology and Innovation Program of Shenzhen (JCYJ20190806144807401), and Grants-in-Aid for Scientific Research (B) JSPS KAKENHI grant nos. JP6H04035 and 16H03949.

REFERENCES

(1) Wang, J. *Nanomachines: Fundamentals and Applications*; John Wiley & Sons: Hoboken, NJ, 2013.

(2) Hu, C.; Pané, S.; Nelson, B. J. Soft Micro-and Nanorobotics. *Annu. Rev. Control, Rob., Auton. Syst.* **2018**, *1*, 53−75.

(3) Medina-Sánchez, M.; Magdanz, V.; Guix, M.; Fomin, V. M.; Schmidt, O. G. Swimming Microrobots: Soft, Reconfigurable, and Smart. *Adv. Funct. Mater.* **2018**, *28*, 1707228.

(4) Mallouk, T. E.; Sen, A. Powering Nanorobots. *Sci. Am.* **2009**, *300*, 72−77.

(5) Wang, W.; Duan, W.; Ahmed, S.; Mallouk, T. E.; Sen, A. Small Power: Autonomous Nano-and Micromotors Propelled by Self-Generated Gradients. *Nano Today* **2013**, *8*, 531−554.

(6) Katuri, J.; Ma, X.; Stanton, M. M.; Sánchez, S. Designing Micro-and Nanoswimmers for Specific Applications. *Acc. Chem. Res.* **2017**, *50*, 2−11.

(7) Li, J.; de Ávila, B. E.-F.; Gao, W.; Zhang, L.; Wang, J. Micro/Nanorobots for Biomedicine: Delivery, Surgery, Sensing, and Detoxification. *Sci. Rob.* **2017**, *2*, 6431.

(8) Eskandarloo, H.; Kierulf, A.; Abbaspourrad, A. Nano-and Micromotors for Cleaning Polluted Waters: Focused Review on Pollutant Removal Mechanisms. *Nanoscale* **2017**, *9*, 13850−13863.

(9) Mallory, S. A.; Valeriani, C.; Cacciuto, A. An Active Approach to Colloidal Self-Assembly. *Annu. Rev. Phys. Chem.* **2018**, *69*, 59−79.

(10) Jin, D.; Yu, J.; Yuan, K.; Zhang, L. Mimicking the Structure and Function of Ant Bridges in a Reconfigurable Microswarm for Electronic Applications. *ACS Nano* **2019**, *13*, 5999−6007.

(11) Xie, H.; Sun, M.; Fan, X.; Lin, Z.; Chen, W.; Wang, L.; Dong, L.; He, Q. Reconfigurable Magnetic Microrobot Swarm: Multimode Transformation, Locomotion, and Manipulation. *Sci. Rob.* **2019**, *4*, No. eaav8006.

(12) Aubret, A.; Youssef, M.; Sacanna, S.; Palacci, J. Targeted Assembly and Synchronization of Self-Spinning Microgears. *Nat. Phys.* **2018**, *14*, 1114.

(13) Savoie, W.; Berrueta, T. A.; Jackson, Z.; Pervan, A.; Warkentin, R.; Li, S.; Murphey, T. D.; Wiesenfeld, K.; Goldman, D. I. A Robot Made of Robots: Emergent Transport and Control of a Smarticle Ensemble. *Sci. Rob.* **2019**, *4*, No. eaax4316.

(14) De Monte, S.; d'Ovidio, F.; Danø, S.; Sørensen, P. G. Dynamical Quorum Sensing: Population Density Encoded in Cellular Dynamics. *Proc. Natl. Acad. Sci. U. S. A.* **2007**, *104*, 18377−18381.

(15) Buck, J. Synchronous Rhythmic Flashing of Fireflies. Ii. *Q. Rev. Biol.* **1988**, *63*, 265−289.

(16) Buck, J.; Buck, E. Biology of Synchronous Flashing of Fireflies. *Nature* **1966**, *211*, 562−564.

(17) DeHaan, R.; Hirakow, R. Synchronization of Pulsation Rates in Isolated Cardiac Myocytes. *Exp. Cell Res.* **1972**, *70*, 214−220.

(18) Nitsan, I.; Drori, S.; Lewis, Y. E.; Cohen, S.; Tzlil, S. Mechanical Communication in Cardiac Cell Synchronized Beating. *Nat. Phys.* **2016**, *12*, 472.

(19) Martens, E. A.; Thutupalli, S.; Fourrière, A.; Hallatschek, O. Chimera States in Mechanical Oscillator Networks. *Proc. Natl. Acad. Sci. U. S. A.* **2013**, *110*, 10563−10567.

(20) Colombano, M.; Arregui, G.; Capuj, N.; Pitanti, A.; Maire, J.; Griol, A.; Garrido, B.; Martínez, A.; Sotomayor-Torres, C. M.; Navarro-Urrios, D. Synchronization of Optomechanical Nanobeams by Mechanical Interaction. *Phys. Rev. Lett.* **2019**, *123*, 017402.

(21) Avnir, D. Chemically Induced Pulsations of Interfaces: The Mercury Beating Heart. *J. Chem. Educ.* **1989**, *66*, 211.

(22) Verma, D. K.; Singh, H.; Parmananda, P.; Contractor, A.; Rivera, M. Kuramoto Transition in an Ensemble of Mercury Beating Heart Systems. *Chaos* **2015**, *25*, 064609.

(23) Lin, S.-W.; Keizer, J.; Rock, P. A.; Stenschke, H. On the Mechanism of Oscillations in the "Beating Mercury Heart. *Proc. Natl. Acad. Sci. U. S. A.* **1974**, *71*, 4477−4481.

(24) Toiya, M.; González-Ochoa, H. O.; Vanag, V. K.; Fraden, S.; Epstein, I. R. Synchronization of Chemical Micro-Oscillators. *J. Phys. Chem. Lett.* **2010**, *1*, 1241−1246.

(25) Cobb, S.; Buhl, E.; Halasy, K.; Paulsen, O.; Somogyi, P. Synchronization of Neuronal Activity in Hippocampus by Individual GABAergic Interneurons. *Nature* **1995**, *378*, 75−78.

(26) Ibele, M.; Mallouk, T. E.; Sen, A. Schooling Behavior of Light-Powered Autonomous Micromotors in Water. *Angew. Chem., Int. Ed.* **2009**, *48*, 3308−3312.

(27) Duan, W.; Liu, R.; Sen, A. Transition between Collective Behaviors of Micromotors in Response to Different Stimuli. *J. Am. Chem. Soc.* **2013**, *135*, 1280−1283.
(28) Ibele, M. E.; Lammert, P. E.; Crespi, V. H.; Sen, A. Emergent, Collective Oscillations of Self-Mobile Particles and Patterned Surfaces under Redox Conditions. *ACS Nano* **2010**, *4*, 4845−4851.
(29) Altemose, A.; Sánchez-Farrán, M. A.; Duan, W.; Schulz, S.; Borhan, A.; Crespi, V. H.; Sen, A. Chemically-Controlled Spatiotemporal Oscillations of Colloidal Assemblies. *Angew. Chem.* **2017**, *129*, 7925−7929.
(30) Altemose, A.; Harris, A. J.; Sen, A. Autonomous Formation and Annealing of Colloidal Crystals Induced by Light-Powered Oscillations of Active Particles. *ChemSystemsChem.* **2020**, *2*, No. e1900021.
(31) Zhou, C.; Chen, X.; Han, Z.; Wang, W. Photochemically Excited, Pulsating Janus Colloidal Motors of Tunable Dynamics. *ACS Nano* **2019**, *13*, 4064−4072.
(32) Zhou, C.; Zhang, H.; Tang, J.; Wang, W. Photochemically Powered AgCl Janus Micromotors as a Model System to Understand Ionic Self-Diffusiophoresis. *Langmuir* **2018**, *34*, 3289−3295.
(33) Wang, W.; Li, S.; Mair, L.; Ahmed, S.; Huang, T. J.; Mallouk, T. E. Acoustic Propulsion of Nanorod Motors inside Living Cells. *Angew. Chem., Int. Ed.* **2014**, *53*, 3201−3204.
(34) Wei, M.; Zhou, C.; Tang, J.; Wang, W. Catalytic Micromotors Moving near Polyelectrolyte-Modified Substrates: The Roles of Surface Charges, Morphology, and Released Ions. *ACS Appl. Mater. Interfaces* **2018**, *10*, 2249−2252.
(35) Wang, W.; Castro, L. A.; Hoyos, M.; Mallouk, T. E. Autonomous Motion of Metallic Microrods Propelled by Ultrasound. *ACS Nano* **2012**, *6*, 6122−6132.
(36) Velegol, D.; Garg, A.; Guha, R.; Kar, A.; Kumar, M. Origins of Concentration Gradients for Diffusiophoresis. *Soft Matter* **2016**, *12*, 4686−4703.
(37) Ibrahim, Y.; Liverpool, T. B. The Dynamics of a Self-Phoretic Janus Swimmer near a Wall. *Europhys. Lett.* **2015**, *111*, 48008.
(38) Chiang, T.-Y.; Velegol, D. Localized Electroosmosis (LEO) Induced by Spherical Colloidal Motors. *Langmuir* **2014**, *30*, 2600−2607.
(39) Kline, T. R.; Paxton, W. F.; Wang, Y.; Velegol, D.; Mallouk, T. E.; Sen, A. Catalytic Micropumps: Microscopic Convective Fluid Flow and Pattern Formation. *J. Am. Chem. Soc.* **2005**, *127*, 17150−17151.
(40) Moo, J. G. S.; Mayorga-Martinez, C. C.; Wang, H.; Teo, W. Z.; Tan, B. H.; Luong, T. D.; Gonzalez-Avila, S. R.; Ohl, C. D.; Pumera, M. Bjerknes Forces in Motion: Long-Range Translational Motion and Chiral Directionality Switching in Bubble-Propelled Micromotors *via* an Ultrasonic Pathway. *Adv. Funct. Mater.* **2018**, *28*, 1702618.
(41) Gröschl, M. Ultrasonic Separation of Suspended Particles-Part I: Fundamentals. *Acta Acust. Acust.* **1998**, *84*, 432−447.
(42) Woodside, S. M.; Bowen, B. D.; Piret, J. M. Measurement of Ultrasonic Forces for Particle-Liquid Separations. *AIChE J.* **1997**, *43*, 1727−1736.
(43) Lee, K. J.; Cox, E. C.; Goldstein, R. E. Competing Patterns of Signaling Activity in Dictyostelium Discoideum. *Phys. Rev. Lett.* **1996**, *76*, 1174.
(44) Aldridge, J.; Pye, E. K. Cell Density Dependence of Oscillatory Metabolism. *Nature* **1976**, *259*, 670−671.
(45) Taylor, A. F.; Tinsley, M. R.; Wang, F.; Huang, Z.; Showalter, K. Dynamical Quorum Sensing and Synchronization in Large Populations of Chemical Oscillators. *Science* **2009**, *323*, 614−617.
(46) Tinsley, M. R.; Taylor, A. F.; Huang, Z.; Wang, F.; Showalter, K. Dynamical Quorum Sensing and Synchronization in Collections of Excitable and Oscillatory Catalytic Particles. *Phys. D* **2010**, *239*, 785−790.
(47) Suematsu, N. J.; Tateno, K.; Nakata, S.; Nishimori, H. Synchronized Intermittent Motion Induced by the Interaction between Camphor Disks. *J. Phys. Soc. Jpn.* **2015**, *84*, 034802.
(48) Kiss, I. Z.; Zhai, Y.; Hudson, J. L. Emerging Coherence in a Population of Chemical Oscillators. *Science* **2002**, *296*, 1676−1678.
(49) Imbihl, R. Nonlinear Dynamics on Catalytic Surfaces: The Contribution of Surface Science. *Surf. Sci.* **2009**, *603*, 1671−1679.
(50) Epstein, I. R.; Pojman, J. A. *An Introduction to Nonlinear Chemical Dynamics: Oscillations, Waves, Patterns, and Chaos*; Oxford University Press: New York, 1998.
(51) Kapral, R.; Showalter, K. *Chemical Waves and Patterns*; Springer Science & Business Media: Berlin, 2012.
(52) Strogatz, S. H. From Kuramoto to Crawford: Exploring the Onset of Synchronization in Populations of Coupled Oscillators. *Phys. D* **2000**, *143*, 1−20.
(53) Iwasa, M.; Iida, K.; Tanaka, D. Various Collective Behavior in Swarm Oscillator Model. *Phys. Lett. A* **2012**, *376*, 2117−2121.
(54) Tanaka, D. General Chemotactic Model of Oscillators. *Phys. Rev. Lett.* **2007**, *99*, 134103.
(55) Prabhakara, K. H.; Gholami, A.; Zykov, V. S.; Bodenschatz, E. Effects of Developmental Variability on the Dynamics and Self-Organization of Cell Populations. *New J. Phys.* **2017**, *19*, 113024.
(56) O'Keeffe, K. P.; Hong, H.; Strogatz, S. H. Oscillators That Sync and Swarm. *Nat. Commun.* **2017**, *8*, 1504.
(57) Hong, Y.; Diaz, M.; Córdova-Figueroa, U. M.; Sen, A. Light-Driven Titanium-Dioxide-Based Reversible Microfireworks and Micromotor/Micropump Systems. *Adv. Funct. Mater.* **2010**, *20*, 1568−1576.
(58) Mou, F.; Zhang, J.; Wu, Z.; Du, S.; Zhang, Z.; Xu, L.; Guan, J. Phototactic Flocking of Photochemical Micromotors. *iScience* **2019**, *19*, 415−424.
(59) Zhou, D.; Gao, Y.; Yang, J.; Li, Y. C.; Shao, G.; Zhang, G.; Li, T.; Li, L. Light-Ultrasound Driven Collective "Firework" Behavior of Nanomotors. *Adv. Sci.* **2018**, *5*, 1800122.
(60) Palacci, J.; Sacanna, S.; Steinberg, A. P.; Pine, D. J.; Chaikin, P. M. Living Crystals of Light-Activated Colloidal Surfers. *Science* **2013**, *339*, 936−940.
(61) Singh, D. P.; Choudhury, U.; Fischer, P.; Mark, A. G. Non-Equilibrium Assembly of Light-Activated Colloidal Mixtures. *Adv. Mater.* **2017**, *29*, 1701328.
(62) Goldenberg, L. M.; Wagner, J.; Stumpe, J.; Paulke, B.-R.; Görnitz, E. Simple Method for the Preparation of Colloidal Particle Monolayers at the Water/Alkane Interface. *Langmuir* **2002**, *18*, 5627−5629.

https://dx.doi.org/10.1021/acsnano.9b08421
ACS Nano 2020, 14, 5360−5370